Structural basis for the specific inhibition of heterotrimeric G_q protein by a small molecule

Akiyuki Nishimura[a,1], Ken Kitano[b,1], Jun Takasaki[c], Masatoshi Taniguchi[c], Norikazu Mizuno[a], Kenji Tago[a], Toshio Hakoshima[b,2], and Hiroshi Itoh[a,2]

[a]Signal Transduction Laboratory and [b]Structural Biology Laboratory, Nara Institute of Science and Technology, 8916-5 Takayama, Ikoma, Nara 630-0192, Japan; and [c]Astellas Pharma Inc., 21 Miyukigaoka, Tsukuba, Ibaraki 305-8585, Japan

Edited* by Alfred G. Gilman, University of Texas Southwestern Medical Center, Dallas, TX, and approved June 15, 2010 (received for review March 18, 2010)

Heterotrimeric GTP-binding proteins (G proteins) transmit extracellular stimuli perceived by G protein-coupled receptors (GPCRs) to intracellular signaling cascades. Hundreds of GPCRs exist in humans and are the targets of a large percentage of the pharmaceutical drugs used today. Because G proteins are regulated by GPCRs, small molecules that directly modulate G proteins have the potential to become therapeutic agents. However, strategies to develop modulators have been hampered by a lack of structural knowledge of targeting sites for specific modulator binding. Here we present the mechanism of action of the cyclic depsipeptide YM-254890, which is a recently discovered G_q-selective inhibitor. YM-254890 specifically inhibits the GDP/GTP exchange reaction of α subunit of G_q protein ($G\alpha_q$) by inhibiting the GDP release from $G\alpha_q$. X-ray crystal structure analysis of the $G\alpha_q\beta\gamma$–YM-254890 complex shows that YM-254890 binds the hydrophobic cleft between two interdomain linkers connecting the GTPase and helical domains of the $G\alpha_q$. The binding stabilizes an inactive GDP-bound form through direct interactions with switch I and impairs the linker flexibility. Our studies provide a novel targeting site for the development of small molecules that selectively inhibit each Gα subunit and an insight into the molecular mechanism of G protein activation.

G protein | crystal structure | specific inhibitor

Heterotrimeric guanine nucleotide-binding proteins (G proteins) serve as critical relays that transmit extracellular stimuli perceived by G protein-coupled receptors (GPCRs) at the cell surface to intracellular signaling cascades (1–3). Heterotrimeric G proteins comprise three subunits, α, β, and γ. The Gα subunit conserves the Ras-like GTPase domain that is essential for hydrolyzing GTP to GDP. In an in vivo resting state, the Gα subunit usually exists in the GDP-bound state and forms a trimer with the β and γ subunits. A ligand-activated GPCR acts as a guanine nucleotide exchange factor (GEF) that stimulates exchange of bound GDP for GTP on the Gα subunit. GTP binding alters three flexible regions, switches I, II, and III, of Gα, leading to Gβγ dissociation and the subsequent binding of Gα and Gβγ to downstream effectors. Signal termination is achieved by GTP hydrolysis, resulting in the reformation of an inactive heterotrimer.

GPCR-mediated signal transduction controls a wide variety of organ functions through multiple signaling pathways (3). The 15 human genes encoding Gα subunits are categorized into four subfamilies: $G\alpha_s$, $G\alpha_I$, $G\alpha_q$, and $G\alpha_{12}$. The multiplicity of receptor-G protein interactions makes it difficult to analyze the intracellular signaling network. The most straightforward approach is to apply a specific inhibitor or activator for one type of G protein. However, until now, availability of small molecules has been limited to a subset of Gα subunits. Strategies to develop small molecule inhibitors have been hampered by a lack of structural information about the inhibitor binding site on the molecular surface.

To identify such an inhibitor binding site, we focused our studies on the cyclic depsipeptide YM-254890, which was isolated from *Chromobacterium* sp. QS3666 as an inhibitor of ADP-induced platelet aggregation (4). YM-254890 strongly inhibits intracellular calcium ion mobilization and serum response element (SRE)-mediated transcription stimulated by several receptors coupled to G_q, but not those coupled to G_i, G_s, or G_{15} (5). YM-254890 also exhibited antithrombotic and thrombolytic effects in an electrically induced carotid artery thrombosis model in rats (6). YM-254890 is the first and only compound that specifically inhibits G_q signaling. Accordingly, it is an invaluable tool for analyzing G protein activation and G_q-mediated cell responses. However, the details of the inhibitory mechanism of YM-254890 remain to be revealed.

In this study, we carried out the biochemical characterization of YM-254890 using purified G proteins in vitro and determined the X-ray crystal structure of the heterotrimeric G_q protein complexed with YM-254890. Our results revealed a unique inhibitory mechanism by which YM-254890 selectively blocks GDP release from the G_q protein.

Results

Specific Inhibition of G_q Family Members by YM-254890. Previously, it was reported that YM-254890 blocks agonist-induced GTPγS binding to $G_{q/11}$ in crude cell membranes (5). This finding suggests the possibility that YM-254890 directly binds to $G\alpha_q$ and inhibits the GDP/GTP exchange. To test this, we first performed an in vitro [^{35}S]GTPγS binding assay using purified $G\alpha_q$ protein. YM-254890 blocked spontaneous GTPγS binding to $G\alpha_q$ in a concentration-dependent manner, suggesting a stoichiometric interaction between $G\alpha_q$ and YM-254890 (Fig. 1 *A* and *B*). On the other hand, YM-254890 had no effect on the spontaneous GTPγS binding to $G\alpha_s$, $G\alpha_{i1}$, $G\alpha_o$, and $G\alpha_{13}$ (Fig. S1). GTP binding to GDP-bound Gα consists of two reactions: dissociation of bound GDP and binding of GTP to nucleotide-free Gα. The dissociation of GDP is a rate-limiting step in the GDP/GTP exchange reaction. We investigated the effect of YM-254890 on GDP dissociation from $G\alpha_q$. [^{3}H]GDP was preloaded on $G\alpha_q$, and [^{3}H]GDP released from $G\alpha_q$ was analyzed in the presence or absence of YM-254890. YM-254890 blocked GDP dissociation from $G\alpha_q$ in a concentration-dependent manner (Fig. 1 *C* and *D*), indicating that YM-254890 acts as a $G\alpha_q$-specific guanine nucleotide dissociation inhibitor (GDI).

Aluminum fluoride (AlF_4^-) is known to activate Gα proteins by mimicking the γ-phosphate of GTP in the presence of GDP (7, 8). Thus, the addition of AlF_4^- induces conformational

Author contributions: A.N., K.K., T.H., and H.I. designed research; A.N., K.K., N.M., and K.T. performed research; J.T. and M.T. contributed new reagents/analytic tools; A.N., K.K., T.H., and H.I. analyzed data; and A.N., K.K., T.H., and H.I. wrote the paper.

The authors declare no conflict of interest.

*This Direct Submission article had a prearranged editor.

Data deposition: The atomic coordinates and structure factors have been deposited in the Protein Data Bank, www.pdb.org (PDB ID code 3AH8).

[1]A.N. and K.K. contributed equally to this work.

[2]To whom correspondence may be addressed. E-mail: hitoh@bs.naist.jp or hakosima@bs.naist.jp.

This article contains supporting information online at www.pnas.org/lookup/suppl/doi:10.1073/pnas.1003553107/-/DCSupplemental.

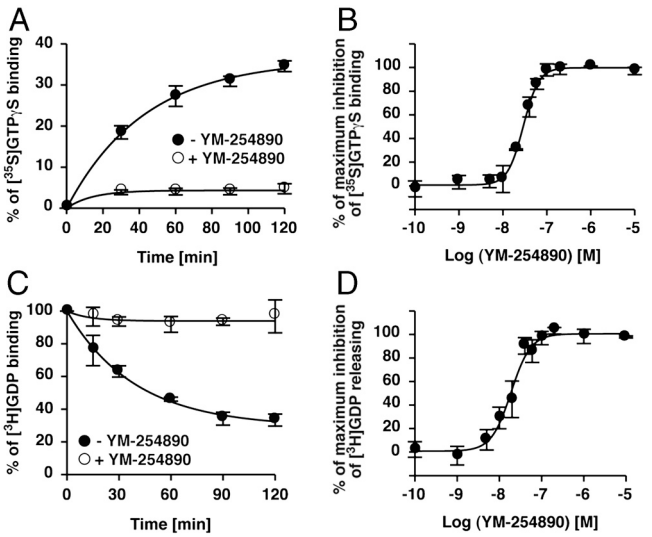

Fig. 1. Inhibitory effects of YM-254890. (*A*) Inhibition of GTPγS binding of $G\alpha_q$. Purified $G\alpha_q$ (100 nM) preincubated without (filled circles) or with (open circles) 10 μM YM-254890 was assayed in the presence of 300 mM $(NH_4)_2SO_4$. (*B*) Dose-dependent inhibition of GTPγS binding to $G\alpha_q$. YM-254890-preincubated $G\alpha_q$ was incubated with GTPγS for 120 min. (*C*) Inhibition of GDP dissociation from $G\alpha_q$. [^{3}H]GDP dissociation from $G\alpha_q$ (50 nM) was monitored without (filled circles) or with (open circles) 10 μM YM-254890 in the presence of 500 μM unlabeled GDP. (*D*) Dose-dependent inhibition of GDP dissociation from $G\alpha_q$ (120 min). Each value represents the mean ± S.D. from three independent experiments.

changes in Gα proteins from the GDP-bound inactive form to the GDP-AlF_4^--bound active state (9, 10). YM-254890 inhibited the AlF_4^--induced conformational change in $G\alpha_q$ and $G\alpha_{14}$ but not $G\alpha_{16}$ (Fig. S2). In Fig. S2, we used ectopically expressed Gα proteins in lysates from mammalian cells, because both $G\alpha_{14}$ and $G\alpha_{16}$ proteins were difficult to purify. The results of a previous study (5) and those of our studies indicate that YM-254890 selectively inhibits $G\alpha_q$, $G\alpha_{11}$, and $G\alpha_{14}$ among mammalian Gα members.

To examine whether YM-254890 inhibits $G\alpha_q$ bound to Gβγ, we prepared heterotrimer His-$G\alpha_{i/q}\beta_1\gamma_2$C68S (henceforth, referred to as His-$G\alpha_{i/q}\beta\gamma$), which contains His-$G\alpha_{i/q}$, $G\beta_1$, and non-prenylated His-$G\gamma_2$C68S. $G\alpha_{i/q}$ is a soluble and functional $G\alpha_q$ chimera in which the wild-type N-terminal helix was replaced with that of $G\alpha_{i1}$ (11). We compared the YM-254890 sensitivity of monomeric His-$G\alpha_{i/q}$ and heterotrimeric His-$G\alpha_{i/q}\beta\gamma$ by using the [^{35}S]GTPγS binding assay. YM-254890 inhibited the GTPγS binding to His-$G\alpha_{i/q}\beta\gamma$ as well as Gβγ-free His-$G\alpha_{i/q}$ (Fig. S3).

Overall Structure of Heterotrimeric G Protein Complexed with YM-254890. To clarify the molecular basis of the YM-254890 action, the crystal structure of $G\alpha_{i/q}\beta\gamma$ bound to YM-254890 was determined at a 2.9 Å resolution (Table S1). The structure reveals the heterotrimer in which $G\gamma_2$-bound $G\beta_1$ forms extensive contacts with $G\alpha_{i/q}$, which consists of the N-terminal helix as well as the GTPase and helical domains (Fig. 2*A*). The major α/β interface covers the N-terminal helix and switch II from the GTPase domain, but not the helical domain, of $G\alpha_{i/q}$. GDP binds to a cleft between the GTPase and helical domains without contacting Gβγ. These structural characteristics are basically similar to the other reported G protein heterotrimer structures (12, 13). YM-254890 docks into the cleft between Linker 1 and Switch I (Linker 2), which connect the GTPase and helical domains. To our knowledge, this cleft has never been described as a critical contact site with other molecules, including Gα effectors (11, 14), Gβγ (12, 13), GoLoco (15), GPCRs (16), or GPCR-mimic peptides (17). A structural comparison of our YM-254890-bound $G\alpha_{i/q}\beta\gamma$ with the inhibitor-free heterotrimers containing $G\alpha_{i1}$ or

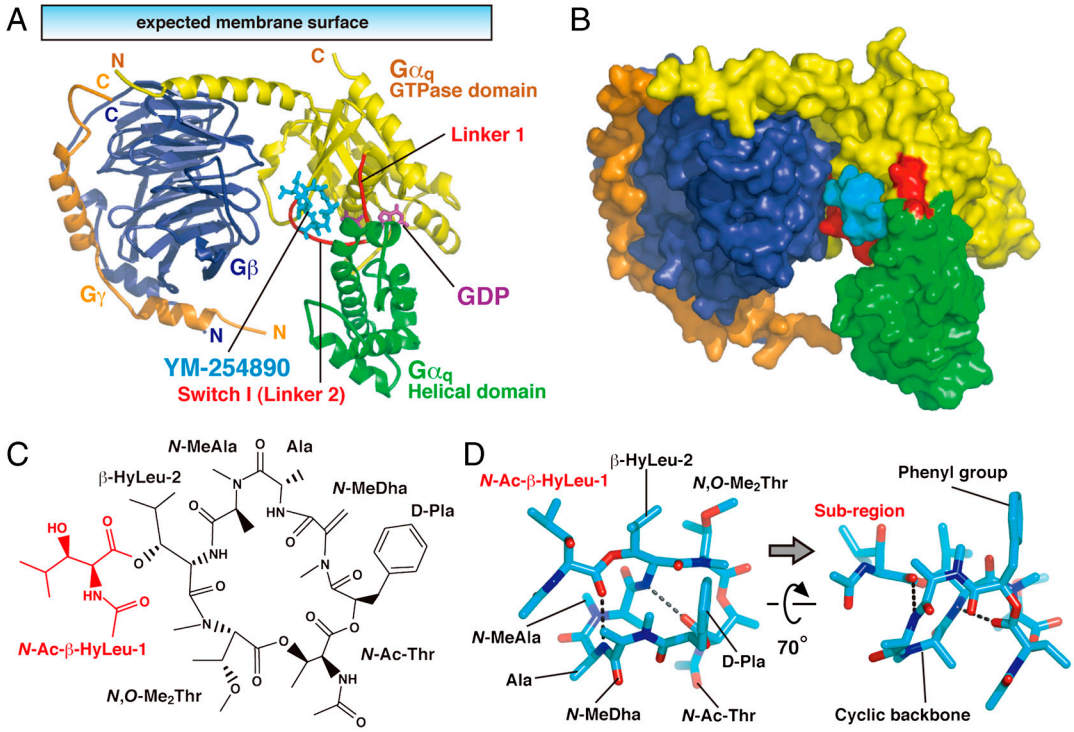

Fig. 2. Overall structure of the $G\alpha_{i/q}\beta\gamma$ heterotrimer in complex with YM-254890. (*A*) The heterotrimer is viewed with the expected orientation at the plasma membrane. $G\alpha_{i/q}$ consists of the GTPase (yellow) and the helical (green) domains connected by two linker regions (red), Linker 1 and Switch I (Linker 2). Gβ and Gγ are blue and orange, respectively. GDP (purple) and YM-254890 (cyan) are shown as stick models. (*B*) Surface representation of the heterotrimer as shown in (*A*). (*C*) Chemical structure of YM-254890. YM-254890 consists of a cyclic backbone (black) and an additional subregion (red). (*D*) Structure model of YM-254890 bound to the heterotrimer. Oxygen and nitrogen are shown in red and blue, respectively. The hydrogen bonds are shown as dashed lines.

$G\alpha_{t/i1}$ (12, 13) suggested a slightly different configuration of the helical domain against the GTPase domain (Fig. S4*A*). Although a crystal packing effect can not be excluded, this rotation of the helical domain relative to the GTPase domain may represent a basic property of $G\alpha_q$ rather than a conformation induced by the binding of YM-254890. The configuration of the two domains of YM-254890-bound $G\alpha_{i/q}$ appears to overlap with the active form of $G\alpha_{i/q}$ (11, 14) (Fig. S4*B*). It is known from the structures of GDP-bound and GTP-bound $G\alpha_t$ that the orientation of the helical domain is unaffected by nucleotide exchange; the structures are quite similar except for the three switch regions. Furthermore, there is precedence for a difference of the configuration of the two domains among Gα subfamilies in the structures reported for $G\alpha_{i1}$ and $G\alpha_t$ (9). Switches I–III of $G\alpha_{i/q}$ preserved the canonical GDP-bound conformation (Fig. S4*C*).

YM-254890 consists of a cyclic backbone and an additional subregion (red region in Fig. 2*C*) with seven amide bonds. YM-254890 in our complex may exhibit a combination of *cis*- or *trans*-amide bond conformations identical to the major conformer suggested by a previous NMR analysis in solution (18) and display an overall conformation of a folded V-shape, which is in part stabilized by intramolecular hydrogen bonds (Fig. 2*D* and Fig. S5). The compact form of YM-254890 has 1047 $Å^2$ of the total solvent accessibility area, of which 52% (543 $Å^2$) is masked by direct contact with $G\alpha_{i/q}$ (Fig. 2*B*).

Binding Mode of YM-254890 to G Protein. The interface between YM-254890 and $G\alpha_{i/q}$ comprises the α1 helix and β2 strand from the GTPase and the αA helix from the helical domains in addition to the two interdomain linkers: Linker 1, connecting the α1 and αA helices, and Switch I (Linker 2), connecting the αF helix and the β2 strand (Fig. 3*A*). The inhibitor–protein interactions are summarized in Fig. 4*A*. Thirteen residues of the binding cleft participate in nonpolar may contacts with YM-254890. At the bottom of the cleft, the aromatic phenyl group of YM-254890 D-Pla docks into a small hydrophobic pocket (Fig. 4*A*) and should make intimate contacts with residues from Switch I (Val^{184} and Thr^{186}) and the GTPase domain (Ile^{56}, Lys^{57}, and Ile^{190}) (Fig. 3 *B* and *C*). To validate the contribution of these resides to the binding affinity, we generated $G\alpha_q$-point mutants and measured the YM-254890 sensitivity of each $G\alpha_q$ mutant. Using the trypsin protection assay, we first confirmed that each $G\alpha_q$ mutant has the capacity to undergo a proper conformation change (Fig. S6). The sensitivity of YM-254890 was evaluated by the SRE-reporter activity induced by the coexpression of the $G\alpha_q$ mutant and the M1 muscarinic acetylcholine receptor. Each substitution of Val^{184} or Ile^{190} to a hydrophilic residue resulted in a marked reduction of YM-254890 sensitivity (940- and 730-fold, respectively) (Fig. 4*B*). Two nonpolar residues (Phe^{75} and Leu^{78}) from the helical domain (αA helix) also contacted YM-254890. The mutation of Leu^{78} exhibited reduction of sensitivity of two orders of magnitude.

YM-254890 may fit its nonpolar side chains of both the subregion and the cyclic peptide to Switch I (Val^{182}-Tyr^{192}), and form two hydrogen bonds to Switch I backbone (Fig. 3*D*). These intimate interactions cannot be retained in the GTP-bound form, whose Switch I is shifted approximately 2 Å away from the YM-254890-bound cleft (19, 20). In sharp contrast to Switch I (Linker 2), Linker 1 lacks most direct contacts with YM-254890. Instead, the salt bridge between Arg^{60} from the GTPase domain (α1 helix) and Asp^{71} from the helical domain (αA helix), the Arg-Asp pair, would mediate the Linker 1-inhibitor interactions by forming multiple hydrogen bonds (Fig. 3*E* and Fig. S7). The terminal guanidium group of Arg^{60} would be essential for these interactions and contribute to the stabilization of the V-shaped ring of the inhibitor. Mutation of Arg^{60} with a lysine residue resulted in approximately 620-fold less sensitivity to YM-254890 (Fig. 4*B*).

Discussion

YM-254890 exhibits exquisite substrate specificity for $G\alpha_q$, $G\alpha_{11}$, and $G\alpha_{14}$. Our sequence alignment reveals that the Gα residues directly interacting with the inhibitor are completely conserved in all YM-254890-sensitive $G\alpha_q$, $G\alpha_{11}$, and $G\alpha_{14}$ but not in other Gα members (Fig. 5). In particular, $G\alpha_{15}$ and $G\alpha_{16}$ conserve all the key residues except Switch I. Our Switch I mutations, I190N

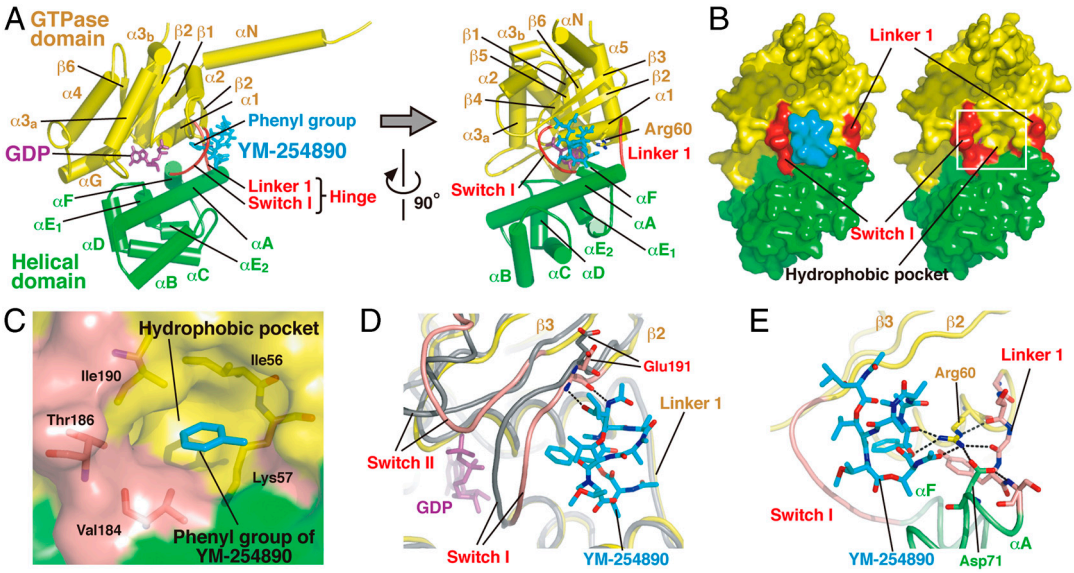

Fig. 3. Specific binding of YM-254890 to $G\alpha_{i/q}$. (*A*) Side and front views of the YM-254890-binding cleft on $G\alpha_{i/q}$ in our complex structure. The key residue Arg^{60} on the α1 helix is shown in a stick model. The color codes are the same as those in Fig. 2*A*. (*B*) Surface representation of the front view of $G\alpha_{i/q}$ with (*Left*) and without (*Right*) YM-254890 to show the pocket between two linkers at the interdomain region. (*C*) Close-up view of the hydrophobic pocket [white square area in (*B*)] that accommodates the phenyl group of YM-254890 (cyan). Residues that form this pocket are depicted as stick models and labeled. The two linkers are pink. (*D*) Switch I-YM-254890 interactions. The inactive GDP-bound form of $G\alpha_{i/q}$ (yellow) in our complex is superimposed on the active form of $G\alpha_q$ (gray) bound to GDP-AlF_4^- and GRK2 (11). Glu^{191} in Switch I is shown as a stick model. The hydrogen bonds between Switch I backbone and the subregion of YM-254890 are shown as dashed lines. The $G\alpha_{i/q}$ switches (pink) are shifted from those of the active form. (*E*) The Arg-Asp pair in Linker 1–YM-254890 interactions. Arg^{60}, Asp^{71}, and Linker 1 residues are shown as stick models. The hydrogen bonds involving the Arg-Asp pair are shown as dashed lines.

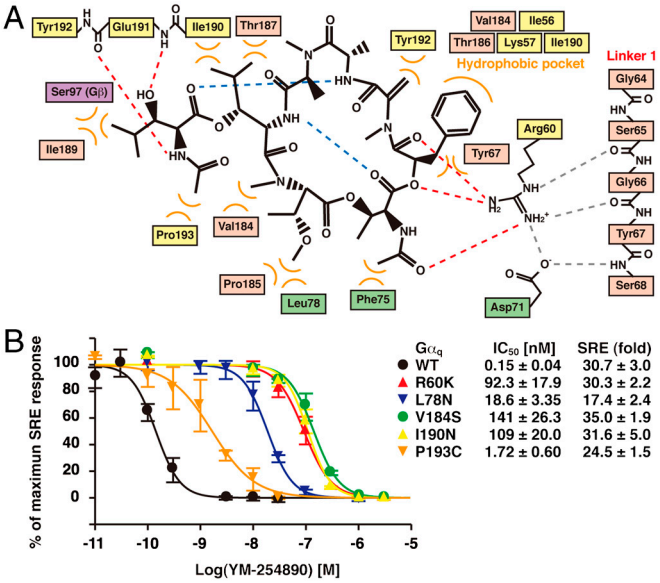

Fig. 4. Summary of the YM-254890–$G\alpha_{i/q}$ interactions and mutation studies. (*A*) Schematic representation of the inhibitor-protein interactions. Intramolecular (blue) and intermolecular (red) hydrogen bonds of YM-254890 are shown as dashed lines. Hydrogen bonds between Arg^{60} and Linker 1 are shown as gray dashed lines. Hydrophobic interactions are indicated as curved orange lines. (*B*) Mutational analysis of $G\alpha_q$ residues that appear to directly interact with YM-254890. YM-254890 sensitivity of each $G\alpha_q$ mutant was evaluated by SRE activation. The calculated IC_{50} values of YM-254890 for each $G\alpha_q$ mutant and SRE activity of each $G\alpha_q$ mutant are shown. Each value represents the mean ± S.D. from three independent experiments performed in duplicate. Mutant protein samples were confirmed to retain proper conformations by the trypsin protection assay (Fig. S6).

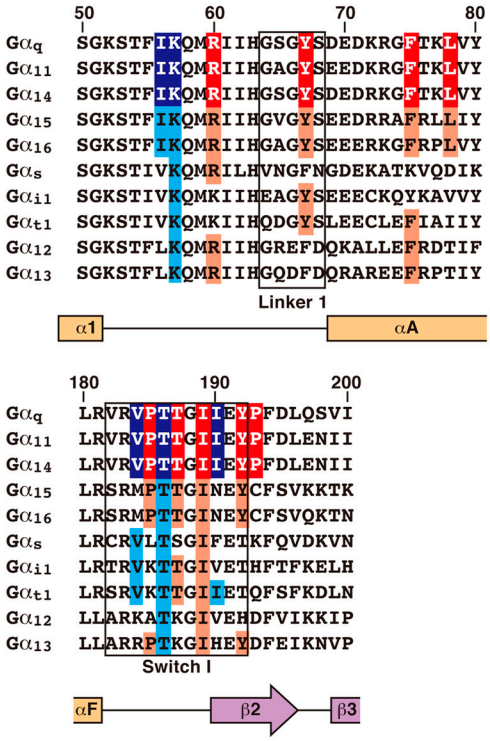

Fig. 5. Sequence alignment of G protein α subunits around the YM-254890 binding site. Linker 1 and Switch I regions are outlined in black. The predicted secondary structure is represented by orange squares and a purple arrow for the α helices and the β strand, respectively. The residue numbering is based on $G\alpha_q$. The residues that appear to directly interact with YM-254890 are shown on a red background. In particular, the residues that form the hydrophobic pocket, which would bind to the phenyl group of YM-254890, are marked with a blue background. Conserved residues at these positions in YM-254890-insensitive Gα are shown on a light-red or light-blue background. These residues are completely conserved only in YM-254890-sensitive $G\alpha_q$, $G\alpha_{11}$, and $G\alpha_{14}$.

and P193C, which replace each $G\alpha_q$ residue with the corresponding residue in $G\alpha_{15}$ and $G\alpha_{16}$, respectively, reduce inhibitor sensitivity (Fig. 4*B*). Thus, we speculate that, in principle, Switch I would ensure the specificity. Other Gα members display sequence diversity in regions other than Switch I. Such an example is $G\alpha_{i1}$, which possesses lysine instead of the key residue Arg^{60}. The R60K mutation severely reduces the activity, as already described (Fig. 4*B*).

YM-254890-mediated stabilization of both interdomain linkers, Linker 1 and Switch I (Linker 2), directly accounts for the repression of the GDP release from $G\alpha_q$ (Fig. 1 *C* and *D*) and, thereby, the repression of the exchange with GTP (Fig. 1 *A* and *B*). A large body of experimental evidence (16, 21–25) supports the importance of the rearrangement of the GTPase and helical domains of Gα to create the necessary route for GDP dissociation. In particular, two flexible interdomain linkers appear to act together as a hinge during the opening of the helical domain away from the GTPase domain. A site-directed spin-labeling study showed that a ligand-activated GPCR triggers the conformational change in Switch I (21). A previous mutation study also indicated that the flexibility of interdomain linkers controls the GDP release rate of Gα (25). In our structure model, YM-254890 forms a cone-like structure with its phenyl group at the head and was stuck deeply into the cleft between both interdomain linkers. As described above, YM-254890 should stabilize Switch I in the inactive GDP-bound conformation through direct interaction (Fig. 3*D*). The Linker 1–YM-254890 interaction with multiple hydrogen bonds would also contribute to the stabilization of interdomain linkers (Fig. 3*E* and Fig. S7). Thus, YM-254890 may repress GDP release by docking into the cleft to reduce a hinge motion of interdomain linkers that are necessary for the rearrangement of the GTPase and helical domains (Fig. 6 *A* and *C*). In contrast, it has been shown that the GoLoco motif, which is known to exert GDI activity against G_i subfamily members, acts as a "clamp" by contacting both the GTPase and helical domains to restrict the domain rearrangement (Fig. 6 *B* and *D*) (15, 26).

The unique binding mode of YM-254890 to G_q is reminiscent of that of the "interfacial inhibitor," which is an alternative to a competitive inhibitor in the development of innovative therapeutics (27, 28). The interfacial inhibitor binds to two macromolecules (protein–protein or protein–nucleic acid) and forms a dead-end complex. Brefeldin A is a typical interfacial inhibitor that stabilizes the abortive complex of Arf and Arf-GEF, inhibiting Arf activation by its GEF (29). In our current model, YM-254890 binds to a cleft between the GTPase and helical domains within one molecule and restricts the conformational rearrangement of these domains. We propose that YM-254890 should be categorized as a unique type of inhibitor, which fixes a domain–domain interface of one macromolecule by binding to hinge regions connecting two intramolecular domains. In some signal-transduction proteins, the interdomain rearrangement is important for the regulation of their molecular functions. The molecular basis of YM-254890 action provides the possibility that a pocket formed by hinge regions becomes a unique site for inhibitor binding.

More recently, constitutive activation of the heterotrimeric G protein α subunit with somatic mutations has been found in uveal melanoma and blue naevi (30). YM-254890 suppresses the oncogenic mutant-induced transcriptional activation (5), suggesting a potential YM-254890 application in cancer in addition to several other diseases. The nucleotide exchange reaction of some α subunits, $G\alpha_q$, $G\alpha_{i1}$, and $G\alpha_o$, is promoted by Ric-8A (31). Interest-

BIOCHEMISTRY

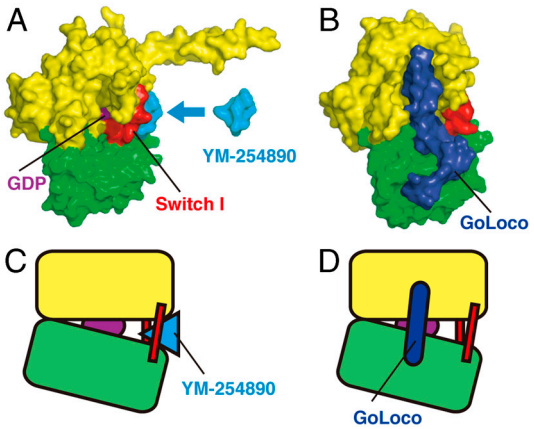

Fig. 6. Comparison of the structural basis for the inhibition of GDP release by YM-254890 and the GoLoco peptide. (*A*) Surface representation of the $G\alpha_{i/q}$–YM-254890 complex (PDB ID: 3AH8). (*B*) Surface representation of the $G\alpha_{i1}$–GoLoco peptide complex (PDB ID: 1KJY). The GoLoco peptide is shown in blue. (*C*) Schematic representation of (*A*). YM-254890 directly inhibits a hinge motion of the helical domain away from the GTPase domain. (*D*) Schematic representation of (*B*). The GoLoco peptide may act as a Gα clamp that restricts the movement of the two domains (14, 25).

ingly, YM-254890 also inhibits the Ric-8A-mediated exchange reaction of $G\alpha_q$ (32), which is consistent with the notion that the inhibitor directly binds to $G\alpha_q$. Cholera (33), pertussis (34), and *Pasturella multocida* (35) toxins are well known modulators of G protein activity. As a G_q-specific inhibitor, YM-254890 should be a useful addition to the tools available to analyze diverse G protein signaling pathways. A close look at the previously reported Gα structures shows that each α subunit preserves the interdomain cleft, which is similar to that of our structure but displays unique surface shapes and properties. This observation suggests that YM-254890 derivatives or YM-254890-mimic compounds could be developed for the specific inhibition of each Gα.

Materials and Methods

Protein Expression and Purification. Baculoviruses encoding His-$G\alpha_{i/q}$ and His-$G\gamma_2$C68S were generated using the Bac-to-Bac baculovirus expression system (Invitrogen). Baculoviruses encoding $G\alpha_q$, $G\alpha_{13}$, $G\beta_1$, and His-$G\gamma_2$ were kindly provided by Tohru Kozasa (University of Illinois at Chicago). Purification of His-$G\alpha_{i/q}$ and $G\alpha_{i/q}\beta_1\gamma_2$C68S from baculovirus-infected High Five cells was performed as previously described (11), with the addition of an anion-exchange chromatography step before a final gel-filtration step. For crystallization, $G\alpha_{i/q}\beta_1\gamma_2$C68S was finally concentrated to 40 mg/mL using Centricon YM-30. Purification of $G\alpha_q$, $G\alpha_{i1}$, and $G\alpha_{13}$ from baculovirus-infected *Sf*9 cells was performed as previously described (36). His-$G\alpha_o$ was purified from BL21(DE3) cells using Ni-NTA agarose (QIAGEN). $G\alpha_s$ was purified from BL21(DE3) cells as previously described (37).

Crystallization. $G\alpha_{i/q}\beta\gamma$ (375 μM, 28 mg/mL) mixed with 2 mM YM-254890 in a buffer containing 20 mM Hepes-NaOH pH 8.0, 100 mM NaCl, 1 mM $MgCl_2$, 2 mM DTT, 0.4 mM GDP, and 4% (v/v) DMSO was used for crystallization. Crystallization screening was carried out by the vapor-diffusion method at 20 °C using commercial screening kits (Nextal Biotechnologies). The protein was mixed in a 1 : 1 ratio with the reservoir solution. Crystallization conditions were subsequently optimized by the sparse matrix method. The prismatic crystal of the $G\alpha_{i/q}\beta\gamma$–YM-254890 complex was obtained under conditions that included 7% PEG 4,000, 70 mM acetate-NaOH pH 5.1, and 30% (v/v) glycerol.

GTPγS Binding Assay. GTPγS binding of the purified Gα was measured using a filter-binding method. The spontaneous GTPγS binding of $G\alpha_q$ and $G\alpha_{i1}$ was promoted in the presence of $(NH_4)_2SO_4$, as previously described (38). Briefly, purified Gα (100 nM) was preincubated with YM-254890 for 3 min at 20 °C in assay buffer A (50 mM Hepes-NaOH pH 7.5, 1 mM EDTA, 1 mM DTT, 0.9 mM $MgSO_4$, and 0.05% Genapol C-100). Reactions were started by the addition of 10 μM [^{35}S]GTPγS (10,000 cpm/pmol) and 300 mM $(NH_4)_2SO_4$. The GTPγS binding of $G\alpha_s$ and $G\alpha_o$ was performed in assay buffer B (20 mM Hepes-NaOH pH 8.0, 100 mM NaCl, 1 mM EDTA, 1 mM DTT, 10 mM $MgSO_4$, and 0.05% Lubrol-PX) (31). The GTPγS binding of $G\alpha_{13}$ was performed in assay buffer C (50 mM Hepes-NaOH pH 7.6, 1 mM EDTA, 1 mM DTT, 0.5 mM $MgSO_4$, and 0.05% Lubrol-PX) (39). Reactions of $G\alpha_q$ and $G\alpha_s$ were carried out at 20 °C, whereas those of $G\alpha_{i1}$, $G\alpha_o$, and $G\alpha_{13}$ were performed at 25 °C. The reactions were stopped by the addition of an ice-cold stop buffer (20 mM Tris-HCl pH 7.7, 100 mM NaCl, 2 mM $MgSO_4$, 0.05% Genapol C-100 or Lubrol-PX, and 1 mM GTP), and the mixtures were filtered through nitrocellulose membranes. The membranes were washed twice with an ice-cold wash buffer (20 mM Tris-HCl pH 7.7, 100 mM NaCl, and 2 mM $MgSO_4$) and air-dried.

GDP Dissociation Assay. $G\alpha_q$ (100 nM) was incubated with 2 μM [^{3}H]GDP (10,000 cpm/pmol) for 18 h at 20 °C in assay buffer A with 50 mM $(NH_4)_2SO_4$. Approximately 25% of $G\alpha_q$ incorporated the radiolabeled nucleotide. The reaction mixtures were then mixed with the same volume of an assay buffer containing an excess of unlabeled GDP (1 mM), DMSO or YM-254890, and 750 mM $(NH_4)_2SO_4$ to monitor the dissociation of [^{3}H]GDP. The reactions were stopped by the addition of an ice-cold wash buffer, and the mixtures were filtered.

Luciferase Assay of the SRE-Mediated Transcription. 293T cells were seeded on a 48-well plate and transfected using Lipofectamine 2000 (Invitrogen) with pCMV5-$G\alpha_q$ or its mutant plasmids (50 – 70 ng/well), pCMV5-M1 muscarinic acetylcholine receptor (10 ng/well), pSRE-Luc (50 ng/well), pEF-RLuc (0.5 ng/well), and pCMV5 up to a total of 300 ng/well of plasmid DNA. YM-254890 was added 20 min after transfection. At 18 h posttransfection, the cells were harvested and subjected to the Dual-Luciferase Reporter Assay System (Promega) using a multilabel plate reader (PerkinElmer). Expression levels of $G\alpha_q$ and its mutants were confirmed by immunoblotting. Firefly luciferase activity derived from pSRE-Luc was normalized to the Renilla luciferase activity derived from pEF-RLuc.

For more information, see *SI Materials and Methods*.

ACKNOWLEDGMENTS. We thank T. Kozasa (University of Illinois at Chicago) for the gift of the baculoviruses encoding $G\alpha_q$, $G\alpha_{13}$, $G\beta_1$, and His-$G\gamma_2$; T. Kawano (University of Illinois at Chicago) for technical advice about the purification of the $G\alpha_{i/q}\beta\gamma$ heterotrimer; Y. Sugawara (Osaka University) for helpful discussions; M. Orita (Astellas Pharma) for the docking simulation of $G\alpha_q\beta\gamma$-YM-254890; N. Shimizu, M. Kawamoto, and M. Yamamoto at SPring-8 for their assistance with the synchrotron experiments; J. Tsukamoto [Nara Institute of Science and Technology (NAIST)] for mass spectrometry; Y. Kaziro (Kyoto University) and M. Linder (Cornell University) for reviewing the manuscript; and all of the members of our laboratories at NAIST for helpful discussions. This work was supported by a Ministry of Education, Culture, Sports, Science, and Technology (MEXT) Grant-in-Aid for Scientific Research on Priority Areas (17079006 and 19036013).

1. Gilman AG (1987) G proteins: Transducers of receptor-generated signals. *Annu Rev Biochem* 56:615–649.
2. Kaziro Y, Itoh H, Kozasa T, Nakafuku M, Satoh T (1991) Structure and function of signal-transducing GTP-binding proteins. *Annu Rev Biochem* 60:349–400.
3. Wettschureck N, Offermanns S (2005) Mammalian G proteins and their cell type specific functions. *Physiol Rev* 85:1159–1204.
4. Taniguchi M, et al. (2003) YM-254890, a novel platelet aggregation inhibitor produced by chromobacterium sp. QS3666. *J Antibiot* 56:358–363.
5. Takasaki J, et al. (2004) A novel Galphaq/11-selective inhibitor. *J Biol Chem* 279:47438–47445.
6. Kawasaki T, et al. (2003) Antithrombotic and thrombolytic efficacy of YM-254890, a Gq/11 inhibitor, in a rat model of arterial thrombosis. *Thromb Haemost* 90:406–413.
7. Sternweis PC, Gilman AG (1982) Aluminum: A requirement for activation of the regulatory component of adenylate cyclase by fluoride. *Proc Natl Acad Sci USA* 79:4888–4891.
8. Bigay J, Deterre P, Pfister C, Chabre M (1985) Fluoroaluminates activate transducin-GDP by mimicking the gamma-phosphate of GTP in its binding site. *FEBS Lett* 191:181–185.
9. Coleman DE, et al. (1994) Structures of active conformations of Gi alpha 1 and the mechanism of GTP hydrolysis. *Science* 265:1405–1412.
10. Sondek J, Lambright DG, Noel JP, Hamm HE, Sigler PB (1994) GTPase mechanism of G proteins from the 1.7- Å crystal structure of transducin α-GDP AlF^-_4. *Nature* 372:276–279.
11. Tesmer VM, Kawano T, Shankaranarayanan A, Kozasa T, Tesmer JJ (2005) Snapshot of activated G proteins at the membrane:The Galphaq-GRK2-Gbetagamma complex. *Science* 310:1686–1690.
12. Wall MA, et al. (1995) The structure of the G protein heterotrimer Gi alpha 1 beta 1 gamma 2. *Cell* 83:1047–1058.
13. Lambright DG, et al. (1996) The 2.0 Å crystal structure of a heterotrimeric G protein. *Nature* 379:311–319.

14. Lutz S, et al. (2007) Structure of Galphaq-p63RhoGEF-RhoA complex reveals a pathway for the activation of RhoA by GPCRs. *Science* 318:1923–1927.
15. Kimple RJ, Kimple ME, Betts L, Sondek J, Siderovski DP (2002) Structural determinants for GoLoco-induced inhibition of nucleotide release by Galpha subunits. *Nature* 416:878–881.
16. Oldham WM, Hamm HE (2008) Heterotrimeric G protein activation by G-protein-coupled receptors. *Nat Rev Mol Cell Biol* 9:60–71.
17. Johnston CA, Siderovski DP (2007) Structural basis for nucleotide exchange on G alpha i subunits and receptor coupling specificity. *Proc Natl Acad Sci USA* 104:2001–2006.
18. Taniguchi M, et al. (2004) YM-254890 analogues, novel cyclic depsipeptides with Galpha(q/11) inhibitory activity from chromobacterium sp. QS3666. *Bioorg Med Chem* 12:3125–3133.
19. Lambright DG, Noel JP, Hamm HE, Sigler PB (1994) Structural determinants for activation of the alpha-subunit of a heterotrimeric G protein. *Nature* 369:621–628.
20. Mixon MB, et al. (1995) Tertiary and quaternary structural changes in Gi alpha 1 induced by GTP hydrolysis. *Science* 270:954–960.
21. Oldham WM, Van Eps N, Preininger AM, Hubbell WL, Hamm HE (2007) Mapping allosteric connections from the receptor to the nucleotide-binding pocket of heterotrimeric G proteins. *Proc Natl Acad Sci USA* 104:7927–7932.
22. Remmers AE, Engel C, Liu M, Neubig RR (1999) Interdomain interactions regulate GDP release from heterotrimeric G proteins. *Biochemistry* 38:13795–13800.
23. Gales C, et al. (2006) Probing the activation-promoted structural rearrangements in preassembled receptor-G protein complexes. *Nat Struct Mol Biol* 13:778–786.
24. Ceruso MA, Periole X, Weinstein H (2004) Molecular dynamics simulations of transducin:Interdomain and front to back communication in activation and nucleotide exchange. *J Mol Biol* 338:469–481.
25. Majumdar S, Ramachandran S, Cerione RA (2004) Perturbing the linker regions of the alpha-subunit of transducin: A new class of constitutively active GTP-binding proteins. *J Biol Chem* 279:40137–40145.
26. Kimple RJ, Willard FS, Siderovski DP (2002) The GoLoco motif: Heralding a new tango between G protein signaling and cell division. *Mol Interv* 2:88–100.
27. Arkin MR, Wells JA (2004) Small-molecule inhibitors of protein-protein interactions: Progressing towards the dream. *Nat Rev Drug Discov* 3:301–317.
28. Pommier Y, Cherfils J (2005) Interfacial inhibition of macromolecular interactions: Nature's paradigm for drug discovery. *Trends Pharmacol Sci* 26:138–145.
29. Renault L, Guibert B, Cherfils J (2003) Structural snapshots of the mechanism and inhibition of a guanine nucleotide exchange factor. *Nature* 426:525–530.
30. Van Raamsdonk CD, et al. (2009) Frequent somatic mutations of GNAQ in uveal melanoma and blue naevi. *Nature* 457:599–602.
31. Tall GG, Krumins AM, Gilman AG (2003) Mammalian ric-8A (synembryn) is a heterotrimeric Galpha protein guanine nucleotide exchange factor. *J Biol Chem* 278:8356–8362.
32. Nishimura A, et al. (2006) Ric-8A potentiates Gq-mediated signal transduction by acting downstream of G protein-coupled receptor in intact cells. *Genes Cells* 11:487–498.
33. Cassel D, Pfeuffer T (1978) Mechanism of cholera toxin action: Covalent modification of the guanyl nucleotide-binding protein of the adenylate cyclase system. *Proc Natl Acad Sci USA* 75:2669–2673.
34. Katada T, Ui M (1982) Direct modification of the membrane adenylate cyclase system by islet-activating protein due to ADP-ribosylation of a membrane protein. *Proc Natl Acad Sci USA* 79:3129–3133.
35. Wilson BA, Ho M (2004) Pasteurella multocida toxin as a tool for studying Gq signal transduction. *Rev Physiol Biochem Pharmacol* 152:93–109.
36. Kozasa T (2004) Purification of G protein subunits from Sf9 insect cells using hexahistidine-tagged alpha and beta gamma subunits. *Methods Mol Biol* 237:21–38.
37. Itoh H, Gilman AG (1991) Expression and analysis of Gs alpha mutants with decreased ability to activate adenylylcyclase. *J Biol Chem* 266:16226–16231.
38. Chidiac P, Markin VS, Ross EM (1999) Kinetic control of guanine nucleotide binding to soluble Galpha(q). *Biochem Pharmacol* 58:39–48.
39. Singer WD, Miller RT, Sternweis PC (1994) Purification and characterization of the alpha subunit of G13. *J Biol Chem* 269:19796–19802.